Theoretical Study of Alkaline-Earth Metal (Be, Mg, and Ca)-Substituted Aluminum Nitride Nanocages With High Stability and Large Nonlinear Optical Responses

Hui-Min He[1], Hui Yang[2]*, Ying Li[3] and Zhi-Ru Li[3]

[1]Department of Physics, Institute of Computational and Applied Physics, Taiyuan Normal University, Jinzhong, China, [2]School of Chemistry and Chemical Engineering, Shanxi Datong University, Datong, China, [3]Laboratory of Theoretical and Computational Chemistry, Jilin University, Changchun, China

By replacing one Al or N atom of aluminum nitride nanocage $Al_{12}N_{12}$ with an alkaline-earth metal atom, two series of compounds, namely, $M@Al_{12}N_{11}$ and $M@Al_{11}N_{12}$ (M = Be, Mg, and Ca), were constructed and investigated in theory. The substituted effect of alkaline-earth metal on the geometric structure and electronic properties of $Al_{12}N_{12}$ is studied in detail by density functional theory (DFT) methods. The calculated binding energies, HOMO–LUMO gaps, and VIE values of these compounds reveal that they possess high stability, though the NBO and HOMO analyses show that they are also excess electron compounds. Due to the existence of diffuse excess electrons, these alkaline-earth metal-substituted compounds exhibit larger first hyperpolarizabilities (β_0) than pure $Al_{12}N_{12}$ nanocage. In particular, these considered compounds exhibit satisfactory infrared (IR) (>1800 nm) and ultraviolet (UV) (< 250 nm) transparency. Therefore, these proposed excess electron compounds with high stability may be regarded as potential candidates for new UV and IR NLO molecules.

Keywords: nonlinear optical response (NLO), excess electron compound, aluminum nitride nanocage, first hyperpolarizabilities, density functional theory

INTRODUCTION

Over the past few decades, the design and synthesis of nonlinear optical (NLO) materials with excellent performance have exerted a tremendous fascination on researchers in consideration of their widespread applications in optics and optoelectronics (Marder Seth et al., 1994; Priyadarshy et al., 1996; Nakano et al., 2002; Zhang et al., 2005; Xiao et al., 2008; Xu et al., 2013). Up to now, abundant strategies have been proposed to acquire high-performance NLO materials of the new type, for instance, designing donor–π-conjugated-bridge-acceptor (D–π-A) models (Kanis et al., 1994), decorating or modifying sp²-hybridized carbon nanomaterials (Bai et al., 2013; Muhammad et al., 2013; Yu et al., 2013; Karamanis et al., 2014; Zhou et al., 2014), synthesizing octupolar molecules (Ja Lee et al., 2003), utilizing a multideck sandwich cluster as the building block (Wang et al., 2015), applying the bond length alternation (BLA) theory (Meyers et al., 1994), enhancing push–pull effects (Liu et al., 2010), and doping metal atoms (Di Bella, 2001; Zhong et al., 2012b; Wu et al., 2014), etc. In particular, Chen et al. (2004) and Li et al. (2004) have revealed that the

introduction of loosely bound excess electrons into a molecule is an effective measure to dramatically enhance its NLO response. Therein, the diffuse excess electron is responsible for improved NLO response. Subsequently, a lot of compounds with dispersed excess electrons, namely, excess electron compounds, are designed in theory, and as expected, they exhibit considerable large NLO responses (Zhong et al., 2015).

In previous studies, it has been found that alkali-metal-doped organic complexants exhibit large first hyperpolarizabilities (Chen et al., 2005; Xu et al., 2007; Wang et al., 2012). In these systems, excess electrons are formed when organic complexants push/pull valence electrons of alkali metal atoms. Therefore, such systems were classified as excess electron compounds, where the alkali metal atom acts as the excess electron source. However, the introduction of active alkali metal atoms reduces stability of these compounds. Therefore, selecting the proper excess electron source to achieve new excess electron compounds will be an efficient way to obtain NLO materials with high stability. To achieve this aim, we have used alkaline-earth metal atoms as an electron source to design several types of excess electron compounds (He et al., 2017a; He et al., 2017b; He et al., 2019) with large first hyperpolarizabilities and satisfying stability.

On the other word, fullerene-like hollow nanocages with noncarbon have attracted great attention owing to their special optoelectronic properties in recent years (Golberg et al., 1998; Strout, 2000; Fu et al., 2001; Stafström et al., 2001; Bertolus et al., 2004; Wang et al., 2005; Beheshtian et al., 2011; Ahmadi Peyghan et al., 2012; Beheshtian et al., 2012c). In particular, Group III–V nitrides are the most promising nanoscale materials in various fields. Therefore, a lot of theoretical and experimental studies have been carried out on the Group III-V fullerene-like nanostructures, especially the most significant AlN nanocages because of their high thermal conductivity and chemical stability (Silaghi-Dumitrescu et al., 1996; Oku et al., 2004; Koi et al., 2005; Yang et al., 2005; Zhang and Zhang, 2005; Zope and Dunlap, 2005; Li et al., 2007; Beheshtian et al., 2012a; Liu et al., 2013; Saeedi et al., 2013). *Ab initio* calculations revealed that the $Al_{12}N_{12}$ nanocage is the most stable AlN nanostructure and thereby can be regarded as an ideal inorganic fullerene-like candidate (Wu et al., 2003). Considering the unique structural and electronic structure of this cage, it has been used as an excellent starting material to design NLO molecules. For instance, two inorganic electrides, $M@Al_{12}N_{12}$(M = Li, Na, and K) (Niu et al., 2014) and $M_3O@Al_{12}N_{12}$ (M = Li, Na, and K) (Sun et al., 2016), were achieved by doping alkali metal atoms and superalkali clusters on the $Al_{12}N_{12}$ nanocage, while the $M@Al_{12}N_{11}$ and $M@Al_{11}N_{12}$ compounds were designed by substituting one atom of $Al_{12}N_{12}$ with an alkali-metal atom (Maria et al., 2016). All these $Al_{12}N_{12}$-based excess electron compounds exhibit considerably high NLO responses.

In order to enhance the NLO responses and stability of such $Al_{12}N_{12}$-based compounds, two series of inorganic compounds, $M@Al_{12}N_{11}$ and $M@Al_{11}N_{12}$ (M = Be, Mg, and Ca), were obtained by substituting Al or N atom in the $Al_{12}N_{12}$ with alkaline-earth metal in the current work. We mainly focus on the following issues: 1) Can loosely bound excess electrons that can dramatically enhance molecular NLO response be generated in these proposed inorganic compounds with alkaline-earth substituted? 2) Do these novel compounds possess larger stability and first hyperpolarizability (β_0) than those of previously reported alkali-metal-substituted systems $M@Al_{12}N_{11}$ and $M@Al_{11}N_{12}$ (M = Li, Na, and K)? Our results revealed that these inorganic compounds $M@Al_{12}N_{11}$ and $M@Al_{11}N_{12}$ (M = Be, Mg, and Ca) indeed contain diffuse excess electrons and thus exhibit larger β_0 values than alkali-metal-substituted systems. In particular, These excess electron compounds exhibit excellent infrared (IR) (>1800 nm) and ultraviolet (UV) (˂ 250 nm) transparency for their potential applications with modern laser frequency conversion technology and optical parameter oscillator processes (Zhang et al., 2009; Luo et al., 2014).

COMPUTATIONAL DETAILS

The geometric structures with all real frequencies are obtained by using a combination of Becke's hybrid 3-parameter exchange functional (Becke, 1993a) and Lee–Yang–Parr's correlation function (Lee et al., 1988) (B3LYP). In a previous study, the Pople-type (Bilbrey et al., 2013) basis set 6-31+G(d) was selected because it has been proved to be reliable for the geometry optimization of similar systems (Niu et al., 2014). Natural bond orbital (NBO) analyses, vertical ionization energies (VIE), and binding energy (E_b) calculations were also performed at the B3LYP/6-31+G(d) level. The binding energy of the alkaline-earth metal atom M was calculated using the counterpoise procedure (Alkorta and Elguero, 1999) and is defined as follows: For $M@Al_{12}N_{11}$,

$$E_b = \left(E_{Al_{12}N_{11}} + E_M\right) - E_{M@Al_{12}N_{11}} \tag{1}$$

For $M@Al_{12}N_{11}$,

$$E_b = \left(E_{Al_{11}N_{12}} + E_M\right) - E_{M@Al_{11}N_{12}} \tag{2}$$

The VIE is the energy difference between neutral molecule and cation systems at the neutral optimization geometry (Wang et al., 2012; Bai et al., 2013; Sun et al., 2015; He et al., 2019).
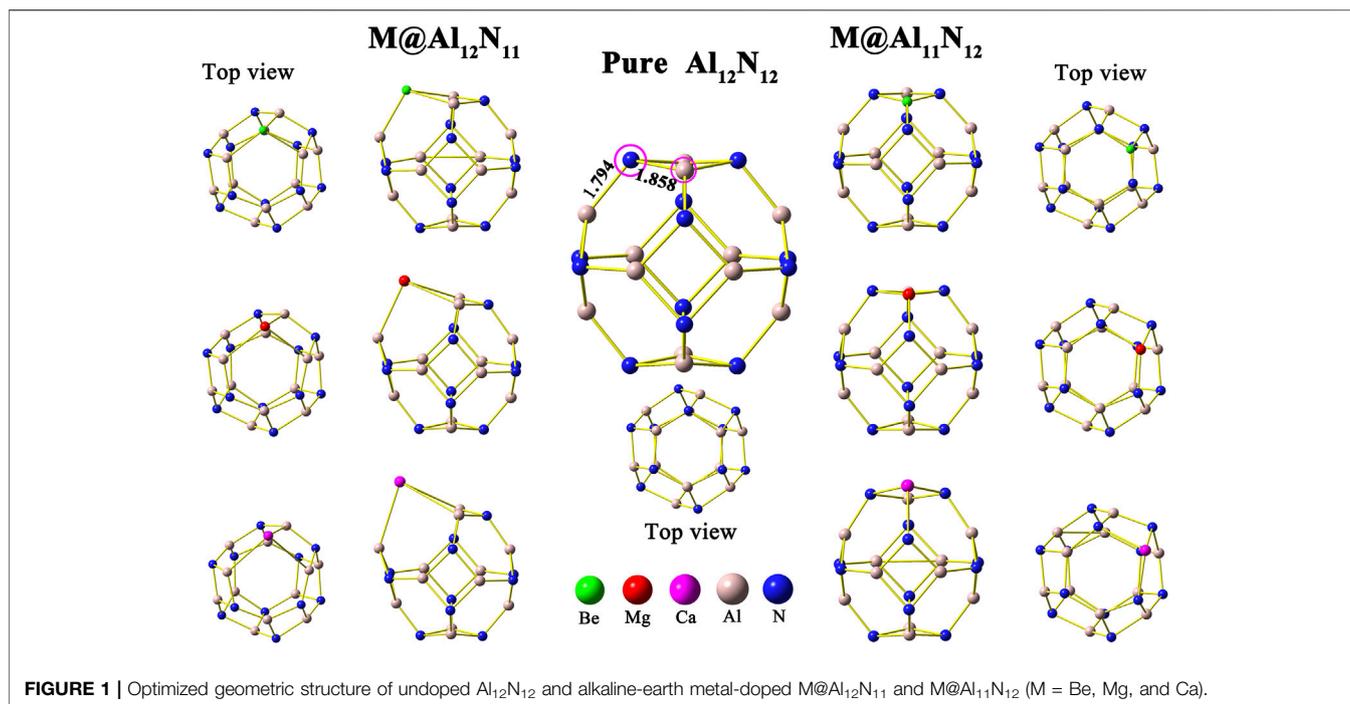
Polarizability and first hyperpolarizability calculations are carried out on long-range correlated methods CAM-B3LYP (Tawada et al., 2004; Yanai et al., 2004) and BHandHLYP (Becke, 1993b) in conjunction with the 6-31+G(d) basis set. As all the systems are in the doublet states, values of spin eigenvalue $\langle S^2 \rangle$ involved in the structural optimization and NLO computations are in the range of 0.760–0.789, which shows an error range of 1.3%–4.9%, indicating that the spin contamination is negligible in the current calculations.

The static polarizability (α_0) and the first hyperpolarizability (β_0) are defined as follows:

$$\alpha_0 = \frac{1}{3}\left(a_{xx} + a_{yy} + a_{zz}\right), \tag{3}$$

$$\beta_0 = \sqrt{\beta_x^2 + \beta_y^2 + \beta_z^2}, \tag{4}$$

where $\beta_i = \frac{3}{5}\left(\beta_{iii} + \beta_{ijj} + \beta_{ikk}\right)$, $i, j, k = x, y, z$.

FIGURE 1 | Optimized geometric structure of undoped $Al_{12}N_{12}$ and alkaline-earth metal-doped $M@Al_{12}N_{11}$ and $M@Al_{11}N_{12}$ (M = Be, Mg, and Ca).

For electronic transition properties, the transition energy ΔE, oscillator strength f_0, and the difference of dipole moment $\Delta \mu$ between the ground and the crucial excited state are estimated by the time-dependent density functional theory, TD-CAM-B3LYP, with the 6-31+G(d) basis set. Simultaneously, ultraviolet-visible–infrared (UV-VIS-IR) absorption spectra of all the systems were also obtained at the same level. All the UV-VIS-IR spectra were reflected with Gaussian curves under a full-width at half-maximum (FWHM) of 0.10 eV.

All of the calculations were carried out by using the Gaussian 16 program package (Frisch et al., 2016). Molecular configurations and molecular orbital (MO) plots were generated with the GaussView program (Dennington et al., 2016).

RESULTS AND DISCUSSION

First, the isolated aluminum nitride nanocage $Al_{12}N_{12}$ was optimized, and its structure is shown in **Figure 1**. In this study, the pure $Al_{12}N_{12}$ nanocage is found to be a T_h-symmetric fullerene-like cage consisting of six 4-membered rings and eight 6-membered rings, in which the Al–N bond lengths are 1.794 and 1.858 Å, respectively, in consistent with earlier reports (Beheshtian et al., 2012a; Beheshtian et al., 2012b; Niu et al., 2014). Then, the initial geometry structures of $M@Al_{12}N_{11}$ and $M@Al_{11}N_{12}$ (M = Be, Mg, and Ca) were constructed by replacing one atom (Al or N) in the $Al_{12}N_{12}$ nanocage with an alkaline-earth metal atom M. In the $M@Al_{12}N_{11}$ series, one alkaline-earth metal atom is substituted for one nitrogen atom, whereas one aluminum atom is replaced with one alkaline-earth metal atom in $M@Al_{11}N_{12}$. After optimization, six equilibrium conformations of $M@Al_{12}N_{11}$ and $M@Al_{11}N_{12}$ have been

TABLE 1 | Symmetry, average M–Al bond length (in Å), average M–N bond length (in Å), HOMO–LUMO gap (H-L Gap, in eV), and vertical ionization energies (VIE, in eV) as well as the binding energy (E_b, in kcal/mol) and NBO charge of alkaline-earth metal atom for $M@Al_{12}N_{11}$ and $M@Al_{11}N_{12}$ (M = Be, Mg, and Ca).

Property	$Al_{12}N_{12}$	$M@Al_{12}N_{11}$			$M@Al_{11}N_{12}$		
		Be	**Mg**	**Ca**	**Be**	**Mg**	**Ca**
Symmetry	T_h	C_s	C_s	C_1	C_s	C_s	C_1
Bond length	1.794/1.858	2.374	2.787	3.206	1.685	2.051	2.385
q^M		-0.358	0.394	0.938	1.101	1.591	1.798
VIE	19.75	6.66	6.22	5.93	8.95	8.80	7.78
E_b		62	33	37	244	163	173
H-L gap	3.84	2.32	2.11	1.73	1.19	1.22	1.19

obtained and are shown in **Figure 1**. The selected geometrical parameters, VIE values, and HOMO–LUMO gap values of these resulting compounds as well as the binding energies and NBO charges of alkaline-earth metal atoms in them are listed in **Table 1**.

As shown in **Table 1**, when one nitrogen or aluminum atom is replaced, the original Al-N bond is elongated. That is to say, the bond lengths of M–Al and M–N in the displaced systems are longer than those of the original Al-N in the pure $Al_{12}N_{12}$ nanocage. Nevertheless, the Be-N bond is a special case in $Be@Al_{11}N_{12}$. The Be-N bond in the $Be@Al_{11}N_{12}$ decreases by ca. 0.175 Å as compared with the Al-N bond in the isolated $Al_{12}N_{12}$ nanocage, which may be attributed to the fact that the nitrogen atom possesses larger electronegativity and the Be atom has smaller atomic radii. It is also found that the bond lengths of M–Al and M–N show a monotonous increase with the increasing atomic number of M. In addition, the M–Al bond length of $M@Al_{12}N_{11}$ series exhibits a larger increment than the M-N bond

FIGURE 2 | HOMOs of $Al_{12}N_{12}$, $M@Al_{12}N_{11}$, and $M@Al_{11}N_{12}$ (M = Be, Mg, and Ca) systems.
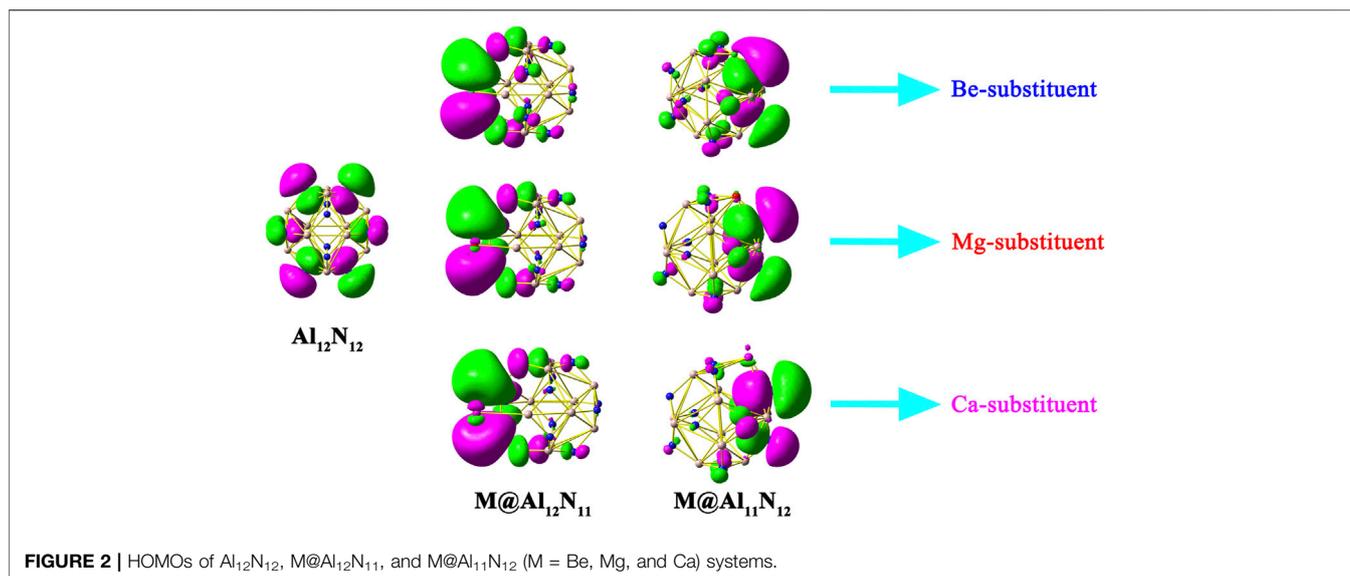
length of the $M@Al_{11}N_{12}$ series as compared with the Al-N bond length of pure $Al_{12}N_{12}$ nanocage.

**Figure 2** displays HOMOs of $Al_{12}N_{12}$ nanocage, $M@Al_{12}N_{11}$, and $M@Al_{11}N_{12}$ (M = Be, Mg, and Ca). It can be seen that the HOMO of a pure $Al_{12}N_{12}$ nanocage consists of p atomic orbitals of N atoms. Differently, all the HOMOs of $M@Al_{12}N_{11}$ and $M@Al_{11}N_{12}$ systems possess diffuse excess electrons, reflecting the unique electric characteristics of these studied compounds. Therefore, these proposed $M@Al_{12}N_{11}$ and $M@Al_{11}N_{12}$ (M = Be, Mg, and Ca) systems can be regarded as a new type of inorganic excess electron compounds. Interestingly, it is found that these systems exhibit almost the same HOMOs.

NBO analysis was carried out to analyze charge transfer in nanocages and electronic structures of these systems. The computed NBO charges on alkaline-earth metal atoms in these studied compounds are given in **Table 1**. From **Table 1**, it can be seen that the NBO charges of alkaline-earth metal atoms in $M@Al_{11}N_{12}$ (M = Be, Mg, and Ca) are in the range of (1.101–1.798) |e|, which is much larger than the charges (0.496–0.788) |e| (Maria et al., 2016) on alkali metal atoms in $M@Al_{11}N_{12}$ (M = Li, Na, and K) and the charges of (0.32-0.60) |e| (Ullah et al., 2020) on alkaline-earth metal atoms in $AEM@Al_{12}N_{12}$ (M = Be, Mg, and Ca), indicating that more charges are transferred from alkaline-earth metal atoms to the nanocages in these compounds. In addition, it is also found that the charges on M atoms in the $M@Al_{11}N_{12}$ series are more electropositive than those of the $M@Al_{12}N_{11}$ series, which may be attributed to the fact that the electronegativity of the nitrogen atom is larger than that of the aluminum atom. When an alkaline-earth metal atom is substituted for an Al atom or N atom, the nitrogen atom has a stronger ability to absorb electrons than the Al atom. Therefore, introducing M atoms in the $M@Al_{11}N_{12}$ series loses more electrons and displays more electropositivity. Additionally, it is found that the charges on M atoms increase along with the increasing M atomic number in both series because of the increasing electropositivity of M. Moreover, the NBO analysis

also reveals that the alkaline-earth metal atoms can serve as the source of diffuse excess electrons for these excess electron compounds.

It is known that the stability of molecules is of great significance for their synthesis in the laboratory and further application in practice. Moreover, the kinetic stability, chemical reactivity, and optical polarizability of any molecule can be described from the energy gap between the highest occupied molecular orbital (HOMO) and the lowest unoccupied molecular orbital (LUMO). HOMO–LUMO gaps of all the studied excess electron compounds are calculated and are summarized in **Table 1**. As can be seen from **Table 1**, pure $Al_{12}N_{12}$ has a large band gap of 3.84 eV, which is a barrier in the way of its applications in electronic devices. As compared with $Al_{12}N_{12}$, a crucial decrease in the HOMO–LUMO gap was noticed for all replaced systems. That is to say, the HOMO–LUMO gaps of $M@Al_{12}N_{11}$ and $M@Al_{11}N_{12}$ are reduced to (1.19–2.32) eV. Even so, the gap values of $M@Al_{12}N_{11}$ (M = Be, Mg, and Ca) compounds are much larger than those (1.39–1.78) eV (Maria et al., 2016) of $M@Al_{12}N_{11}$ (M = Li, Na, and K) compounds, comparable to that (1.57 eV) (Wang et al., 1999) of the kinetically stable C_{60}, and those (1.59–3.79) eV (Ullah et al., 2020) of $AEM@Al_{12}N_{12}$ (M = Be, Mg, and Ca), suggesting the large chemical stability of the studied $M@Al_{12}N_{11}$ (M = Be, Mg, and Ca) species. From **Figure 3**, it is also found that the gap values decrease along with the decreasing M atomic number for the $M@Al_{12}N_{11}$ series, whereas they are hardly equal for the $M@Al_{11}N_{12}$ series.

Furthermore, the large electronic stability of these excess electron compounds can also be characterized by their higher vertical ionized energies (VIEs) of (5.93–8.95) eV, which are slightly higher than the reported values of inorganic and organic excess electron compounds (Chen et al., 2005; Zhong et al., 2012a; He et al., 2017a; He et al., 2017b; Ullah et al., 2020), indicating that these proposed nanocage compounds exhibit high electronic stability. **Figure 3** demonstrates the alkaline-earth metal
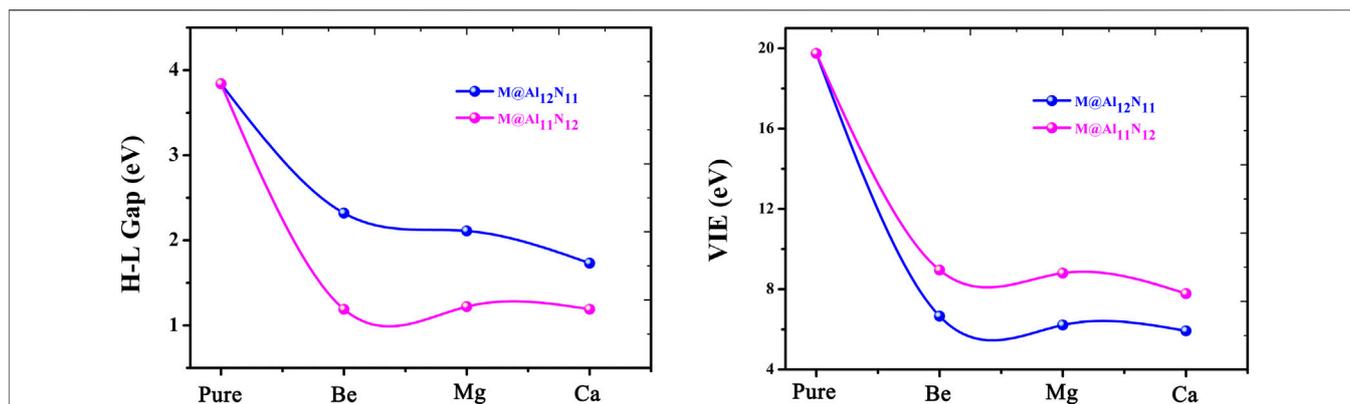
FIGURE 3 | Relationship between H-L Gaps and VIE values with the atomic number of alkaline-earth metals.

TABLE 2 | Static polarizability (α_O), static first hyperpolarizability β_O, oscillator strength (f_o), transition energy (ΔE, in eV), and difference of dipole moment ($\Delta\mu$ in D) between the ground and the crucial excited states and crucial transition for $M@Al_{12}N_{11}$ and $M@Al_{11}N_{12}$ (M = Be, Mg and Ca).

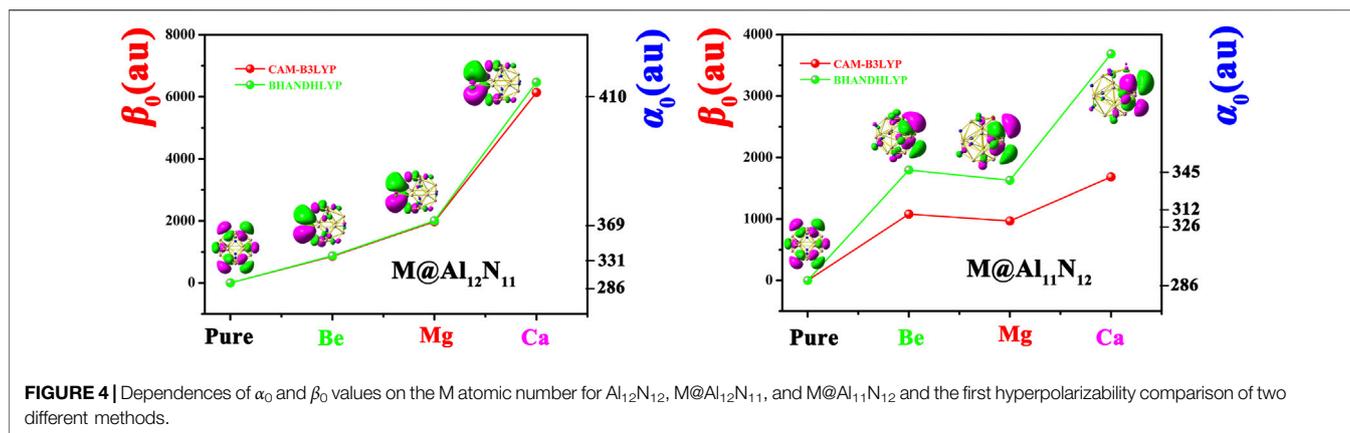|		α_O	$\beta_O{}^a$	$\beta_O{}^b$	f_o	ΔE	$\Delta\mu$	Crucial transition
$Al_{12}N_{12}$	-		286	0	0	0.0176	4.759	0	-
$M@Al_{12}N_{11}$	Be	331	861	875	0.0434	3.32	2.53	$\alpha H \rightarrow \alpha L+3$ (23.8%)
				-				$\alpha H \rightarrow \alpha L+5$ (19.1%)
				-				$\beta H-1 \rightarrow \beta L$ (17.2%)
	Mg	369	1979	2006	0.1034	2.93	2.27	$\alpha H-1 \rightarrow \alpha L+1$ (37.1%)
				-				$\beta H \rightarrow \beta L+2$ (41.2%)
	Ca	410	6,140	6,473	0.0783	2.83	2.19	$\alpha H-1 \rightarrow \alpha L+2$ (18.9%)
								$\alpha H-1 \rightarrow \alpha L+1$ (15.7%)
				-				$\beta H \rightarrow \beta L+2$ (39.7%)
$M@Al_{11}N_{12}$	Be	312	1,079	1796	0.0181	0.77	3.40	$\beta H \rightarrow \beta L$ (87.1%)
	Mg	326	969	1,628	0.0354	0.97	2.53	$\beta H \rightarrow \beta L$ (64.5%)
				-				$\beta H-2 \rightarrow \beta L$ (19%)
	Ca	345	1,683	3,687	0.0420	0.92	2.09	$\beta H \rightarrow \beta L$ (49.6%)
				-				$\beta H-1 \rightarrow \beta L$ (32.7%)

[a]for CAM-B3LYP level.
[b]for BHandHLYP level.

atomic number effect on VIE values, namely, the larger the atomic number, the smaller the VIE value.

Additionally, the binding energies (E_b) of these designed $M@Al_{12}N_{11}$ and $M@Al_{11}N_{12}$ compounds are also calculated and given in **Table 1**. The E_b values are defined as the negative of the intramolecular interaction energies between the alkaline-earth metal M and the remaining $Al_{12}N_{11}$ or $Al_{11}N_{12}$ moieties. Thus, the larger the E_b value is, the stronger the interaction between two subunits. From **Table 1**, it can be seen that all the proposed excess electron compounds exhibit much larger E_b values of (33.0-244.0) kcal/mol than those (31-89 kcal/mol) (Maria et al., 2016) of previously reported alkali-metal substituted compounds, indicating that alkaline-earth metal atoms are more tightly bound to the remaining $Al_{12}N_{11}$ or $Al_{11}N_{12}$ units than the alkali metal atoms in $M@Al_{12}N_{11}$ and $M@Al_{11}N_{12}$ (M = Li, Na, and K). More importantly, the $M@Al_{11}N_{12}$ (M = Be, Mg, and Ca) series exhibit extremely large E_b values up to (173-244) kcal/mol, which are far more than those of (64-89) kcal/mol for $M@Al_{11}N_{12}$ (M = Li, Na, and K) (Maria

et al., 2016). Thus, as compared with alkali metal atoms, the introduction of alkaline-earth metal atoms into the $Al_{12}N_{12}$ nanocage can produce more stable species with excess electrons. In addition, the E_b values of proposed alkaline-earth metal substituted excess electron compounds are also comparable to those (59-106) kcal/mol of small clusters with alkaline-earth metal atoms (Srivastava et al., 2018).

To evaluate nonlinear optical response, the dipole moments (μ_0), polarizabilities (α_0), and first hyperpolarizabilities (β_0) of pure $Al_{12}N_{12}$ and the proposed $M@Al_{12}N_{11}$ and $M@Al_{11}N_{12}$ compounds were calculated and are summarized in **Table 2**. To better visualize the results, the dependences of the polarizability (α_0) and first hyperpolarizability (β_0) values on the alkaline-earth metal atomic number are exhibited in **Figure 4**. Our results revealed that the α_0 (286 au) of the $Al_{12}N_{12}$ nanocage is increased to 319-410 au for replaced compounds, indicating that the substitution of alkaline-earth metal atoms virtually affects the α_0 value of the $Al_{12}N_{12}$ molecule. As shown in **Table 2** and **Figure 4**, the α_0 changes in the order of 331 au (Be) < 369 au (Mg)

FIGURE 4 | Dependences of α_0 and β_0 values on the M atomic number for $Al_{12}N_{12}$, $M@Al_{12}N_{11}$, and $M@Al_{11}N_{12}$ and the first hyperpolarizability comparison of two different methods.

< 410 au (Ca) in the $M@Al_{12}N_{11}$ series and similarly, varies in the order of 312 au (Be) < 326au (Mg) < 345 au (Ca) in the $M@Al_{11}N_{12}$ series. In short, α_0 increases along with the increasing M atomic number. Also, it is observed that the $M@Al_{12}N_{11}$ exhibits a relatively larger α_0 value than the corresponding $M@Al_{11}N_{12}$, indicating that the excess electrons in the HOMOs of the former are more diffuse than the latter because static polarizability is sensitive to electronic delocalization.

Due to the pure $Al_{12}N_{12}$ nanocage being centrosymmetric, its β_0 values are zero. Thus, different from α_0, the substitution of M for Al or N atom in $Al_{12}N_{12}$ brings a prominent improvement of first hyperpolarizability (β_0) of the $Al_{12}N_{12}$ nanocage, which is because that M-substitution not only destroys the centrosymmetry of $Al_{12}N_{12}$ but also makes two kinds of replaced systems possessing the dispersed excess electrons. Two different long-range corrected methods were used to calculate the hyperpolarizability β_0 values, which have been listed in **Table 2**. **Figure 4** manifests the first hyperpolarizability at CAM-B3LYP for $M@Al_{12}N_{11}$ and $M@Al_{11}N_{12}$ follows the same trend as for BHandHLYP. However, the calculated values at CAM-B3LYP are slightly lower than BHandHLYP.

Additionally, it can be distinctly seen from **Table 2** and **Figure 4** that the β_0 values of Ca-substitution compounds are greatly larger than those of Be-substitution and Mg-substitution compounds, signifying an evident effect of the M atomic number on the NLO responses of $M@Al_{12}N_{11}$ and $M@Al_{11}N_{12}$. To be specific, the varying order for β_0 is 861au (Be) < 1979au (Mg) < 6140au (Ca) in the $M@Al_{12}N_{11}$ series, which is consistent with the change sequence of α_0 values. That is, the compounds with higher polarizabilities also present relatively higher NLO responses because of the more diffuse excess electrons in them.

The comparison of β_0 values between our proposed excess electron compounds and previously reported alkali-metal substituted compounds is meaningful. In the $M@Al_{12}N_{11}$ series, it can be seen that reported alkali-metal substituted compounds exhibit much larger β_0 values of (2,500-9,100) au (in CAM-B3LYP/6-311 + g* level) (Maria et al., 2016) than those (861-6,140) au of our proposed alkaline-earth metal substituted excess electron compounds. However, the resultant comparison of β_0 values is inverse in the $M@Al_{11}N_{12}$ series, namely, β_0 values

(1,628–3,687) au of alkaline-earth metal-substituted compounds are larger than those (420–770) kcal/mol of alkali-metal-substituted compounds. Thus, when a N atom is substituted by alkaline-earth metal atoms in an $Al_{12}N_{12}$ nanocage, excess electron compounds $M@Al_{11}N_{12}$ (M = Be, Mg, and Ca) can exhibit larger NLO responses than $M@Al_{11}N_{12}$ (M = Li, Na, and K).

For intensive discernment of this significant increase in first hyperpolarizability due to substitution of alkaline-earth metal in the $Al_{12}N_{12}$ nanocage, let us consider the simplest two-level model (Maroulis, 1996; Xu et al., 2009), which is derived from the sum-over states method:

$$\beta_0 \approx \frac{\Delta\mu f_0}{\Delta E^3}, \tag{5}$$

where involved ΔE, f_0, and $\Delta\mu$ are the transition energy, oscillator strength, and difference of the dipole moment between the ground state and the crucial excited state, respectively. The expression distinctly displays that β_0 is inversely proportional to the third power of ΔE. Therefore, crucial transition energy plays an important role in the evaluation of β_0. In the current work, the TD-CAM-B3LYP calculations are performed to obtain the dominated excited states of these studied compounds. The crucial transitions and the corresponding ΔE, f_0, and $\Delta\mu$ values are presented in **Table 2** and **Figure 5**, respectively. It is noted that the electrons involved in the crucial excited states of these considered species primarily come from their HOMO, HOMO-1, and HOMO-2 orbitals. Meanwhile, from **Figure 5**, it can be seen that crucial transitions make the electrons more diffuse, which may lead to the large β_0.H

Moreover, compared to the large ΔE value (4.759 eV) in pure $Al_{12}N_{12}$, the $M@Al_{12}N_{11}$ and $M@Al_{11}N_{12}$ compounds exhibit much smaller ΔE values of (0.77-3.32) eV, which are comparable to those of (1.295–1.982) eV for the alkali metal-based electrides, including Li@(calix [4]pyrrole) (Chen et al., 2005), Li_n-H-$(CF_2$-$CH_2)_3$-H (n = 1, 2) (Xu et al., 2007), $H_4C_4N_2 \cdots Na_2$ (Ma et al., 2008), and Li@$B_{10}H_{14}$ (Muhammad et al., 2009), and far less than (4.6–6.7) eV of $M@Al_{12}N_{11}$ and $M@Al_{11}N_{12}$(M = Li, Na, and K) (Maria et al., 2016), as well as (1.80–4.76) eV of $AEM@Al_{12}N_{12}$ (Ullah et al., 2020). Hence, these small ΔE values bring forth the large β_0 values of these proposed alkaline-earth metal-based excess electron compounds.
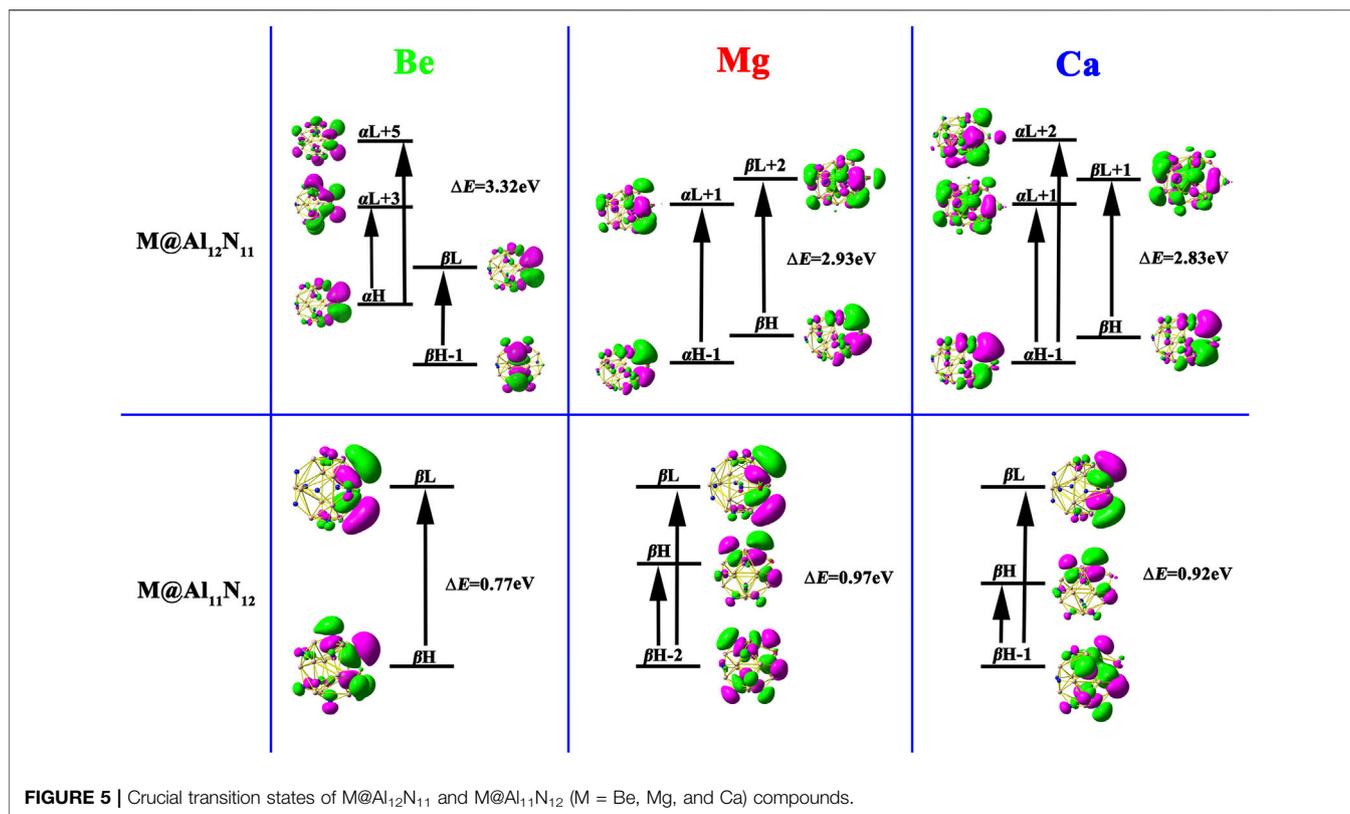
FIGURE 5 | Crucial transition states of $M@Al_{12}N_{11}$ and $M@Al_{11}N_{12}$ (M = Be, Mg, and Ca) compounds.
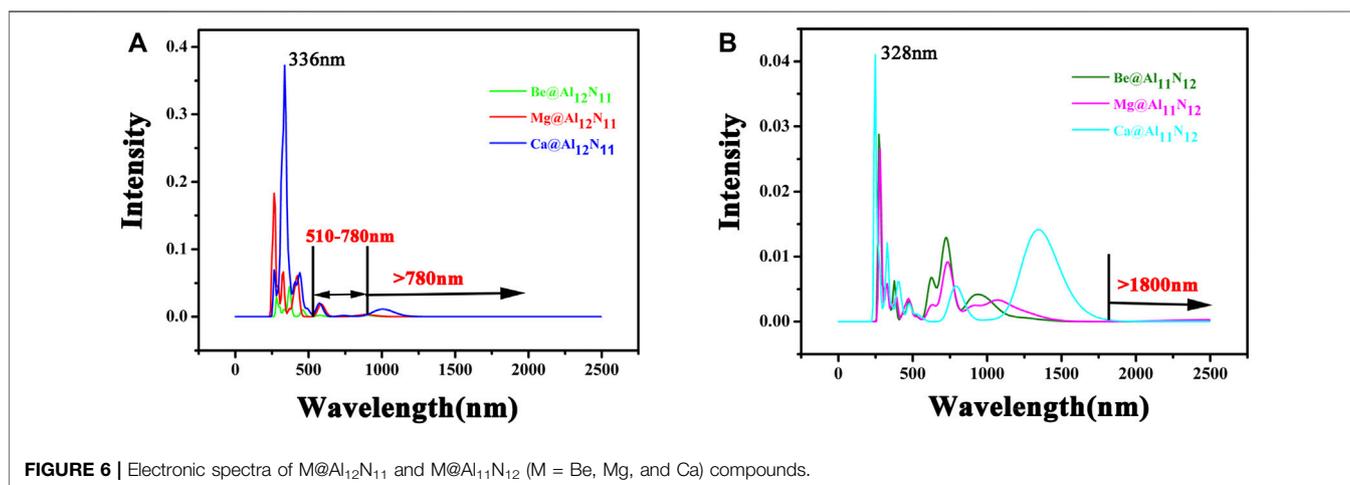
FIGURE 6 | Electronic spectra of $M@Al_{12}N_{11}$ and $M@Al_{11}N_{12}$ (M = Be, Mg, and Ca) compounds.

It is well-known that the main applications for NLO materials are in doubling frequency and second harmonic generation (SHG). Accordingly, the superior NLO materials not only need large NLO response but also must be transparent under the applied laser region. Therefore, the ultraviolet-visible–infrared (UV-VIS-NIR) absorption spectra of these $M@Al_{12}N_{11}$ and $M@Al_{11}N_{12}$ compounds are gained and shown in **Figure 6**. From **Figure 6A**, it can be seen that the main absorption region of $M@Al_{12}N_{11}$ compounds is from 300 to 500 nm. The absorption of these compounds in the infrared spectral region is weak, especially for

$Be@Al_{12}N_{11}$, there is no absorption in the visible region of (510–780) nm and the infrared spectral region, which suggests that $Be@Al_{12}N_{11}$ has satisfying transparency in both the visible region of (510–780) nm and infrared spectral region. In addition, **Figure 6B** shows that the $M@Al_{11}N_{12}$ series have an infrared (IR) transparent region at wavelength >1800 nm. Thus, it is hoped that these six excess electron compounds could be used as new IR NLO materials. Simultaneously, it is observed that they also have an ultraviolet (UV) transparent region at wavelength ˂ 250 nm. Then, they may be taken as a new candidate for UV NLO materials.

CONCLUSIONS

Using the density functional theory (DFT), two new series of excess electron compounds, i.e., $M@Al_{12}N_{11}$ and $M@Al_{11}N_{12}$ (M = Be, Mg, and Ca), have been obtained and studied theoretically in this work. The substituted effect of alkaline-earth metal on the geometric structures and electronic properties of aluminum nitride ($Al_{12}N_{12}$) nanocage has been investigated in detail. Binding energy calculations display that these proposed compounds, particularly the Al-replaced nanocages have high structural stability. In addition, the substitution of alkaline-earth metal for Al and N in $Al_{12}N_{12}$ significantly reduces its HOMO–LUMO gap and VIE value, which may bring forth large optical polarizability. More importantly, these studied compounds contain diffuse excess electrons and thus show high NLO responses. Particularly, our results reveal that all these considered compounds show satisfying infrared (IR) transparent region (>1800 nm) and ultraviolet (UV) region (< 250 nm). Thus, we hope that this study could not only provide new candidates of potential NLO molecules but also promote future applications of Al-N fullerene-like nanocages in the field of nonlinear optics.

REFERENCES

Ahmadi Peyghan, A., Pashangpour, M., Bagheri, Z., and Kamfiroozi, M. (2012). Energetic, Structural, and Electronic Properties of Hydrogenated $Al_{12}P_{12}$ Nanocluster. *Phys. E Low-dimensional Syst. Nanostructures* 44 (7), 1436–1440. doi:10.1016/j.physe.2012.03.007

Alkorta, I., and Elguero, J. (1999). Theoretical Study of Strong Hydrogen Bonds between Neutral Molecules: The Case of Amine Oxides and Phosphine Oxides as Hydrogen Bond Acceptors. *J. Phys. Chem. A* 103 (2), 272–279. doi:10.1021/jp982644n

Bai, Y., Zhou, Z.-J., Wang, J.-J., Li, Y., Wu, D., Chen, W., et al. (2013). New Acceptor-Bridge-Donor Strategy for Enhancing NLO Response with Long-Range Excess Electron Transfer from the $NH_2.M/M_3O$ Donor (M = Li, Na, K) to inside the Electron Hole Cage C20F19 Acceptor through the Unusual σ Chain Bridge $(CH_2)_4$. *J. Phys. Chem. A* 117 (13), 2835–2843. doi:10.1021/jp3120594

Becke, A. D. (1993b). A New Mixing of Hartree-Fock and Local Density-functional Theories. *J. Chem. Phys.* 98 (2), 1372–1377. doi:10.1063/1.464304

Becke, A. D. (1993a). Density-functional Thermochemistry. III. The Role of Exact Exchange. *J. Chem. Phys.* 98 (7), 5648–5652. doi:10.1063/1.464913

Beheshtian, J., Bagheri, Z., Kamfiroozi, M., and Ahmadi, A. (2012a). A Comparative Study on the $B_{12}N_{12}$, $Al_{12}N_{12}$, $B_{12}P_{12}$ and $Al_{12}P_{12}$ Fullerene-like Cages. *J. Mol. Model.* 18 (6), 2653–2658. doi:10.1007/s00894-011-1286-y

Beheshtian, J., Bagheri, Z., Kamfiroozi, M., and Ahmadi, A. (2011). Toxic CO Detection by $B_{12}N_{12}$ Nanocluster. *Microelectron. J.* 42 (12), 1400–1403. doi:10.1016/j.mejo.2011.10.010

Beheshtian, J., Peyghan, A. A., Bagheri, Z., and Kamfiroozi, M. (2012c). Interaction of Small Molecules (NO, H_2, N_2, and CH_4) with BN Nanocluster Surface. *Struct. Chem.* 23 (5), 1567–1572. doi:10.1007/s11224-012-9970-9

Beheshtian, J., Peyghan, A. A., and Bagheri, Z. (2012b). Selective Function of $Al_{12}N_{12}$ Nano-Cage towards NO and CO Molecules. *Comput. Mater. Sci.* 62, 71–74. doi:10.1016/j.commatsci.2012.05.041

Bertolus, M., Finocchi, F., and Millié, P. (2004). Investigating Bonding in Small Silicon-Carbon Clusters: Exploration of the Potential Energy Surfaces of Si_3C_4, Si_4C_3, and Si_4C_4 Using Ab Initio Molecular Dynamics. *J. Chem. Phys.* 120 (9), 4333–4343. doi:10.1063/1.1636717

Bilbrey, J. A., Kazez, A. H., Locklin, J., and Allen, W. D. (2013). Exact Ligand Cone Angles. *J. Comput. Chem.* 34 (14), 1189–1197. doi:10.1002/jcc.23217

Chen, W., Li, Z.-R., Wu, D., Gu, F.-L., Hao, X.-Y., Wang, B.-Q., et al. (2004). The Static Polarizability and First Hyperpolarizability of the Water Trimer anion:Ab Initiostudy. *J. Chem. Phys.* 121 (21), 10489–10494. doi:10.1063/1.1811609

Chen, W., Li, Z.-R., Wu, D., Li, Y., Sun, C.-C., and Gu, F. L. (2005). The Structure and the Large Nonlinear Optical Properties of Li@Calix[4]pyrrole. *J. Am. Chem. Soc.* 127 (31), 10977–10981. doi:10.1021/ja050601w

Dennington, R. D., Keith, T. A., and Millam, J. M. (2016). *GaussView, Version6. Shawnee Mission*. KS: Semichem Inc.

Di Bella, S. (2001). Second-order Nonlinear Optical Properties of Transition Metal Complexes. *Chem. Soc. Rev.* 30 (6), 355–366. doi:10.1039/B100820J

Frisch, M. J., Trucks, G. W., Schlegel, H. B., Scuseria, G. E., Robb, M. A., Cheeseman, J. R., et al. (2016). *Gaussian 16, Revision A.03*. Wallingford CT, USA: Gaussian, Inc.

Fu, C.-C., Weissmann, M., Machado, M., and Ordejón, P. (2001). Ab Initiostudy of Silicon-Multisubstituted Neutral and Charged Fullerenes. *Phys. Rev. B* 63 (8), 085411. doi:10.1103/PhysRevB.63.085411

Golberg, D., Bando, Y., Stéphan, O., and Kurashima, K. (1998). Octahedral Boron Nitride Fullerenes Formed by Electron Beam Irradiation. *Appl. Phys. Lett.* 73 (17), 2441–2443. doi:10.1063/1.122475

He, H.-M., Li, Y., Yang, H., Yu, D., Li, S.-Y., Wu, D., et al. (2017a). Efficient External Electric Field Manipulated Nonlinear Optical Switches of All-Metal Electride Molecules with Infrared Transparency: Nonbonding Electron Transfer Forms an Excess Electron Lone Pair. *J. Phys. Chem. C* 121 (1), 958–968. doi:10.1021/acs.jpcc.6b11919

He, H.-M., Li, Y., Yang, H., Yu, D., Wu, D., Zhong, R.-L., et al. (2017b). Effects of the Cage Number and Excess Electron Number on the Second Order Nonlinear Optical Response in Molecular All-Metal Electride Multicage Chains. *J. Phys. Chem. C* 121 (45), 25531–25540. doi:10.1021/acs.jpcc.7b06464

He, H.-M., Luis, J. M., Chen, W.-H., Yu, D., Li, Y., Wu, D., et al. (2019). Nonlinear optical response of endohedral all-metal electride cages $2e^-Mg^{2+}(M@E^{12})^{2-}Ca^{2+}$ (M = Ni, Pd, and Pt; E = Ge, Sn, and Pb). *J. Mat. Chem. C* 7 (3), 645–653. doi:10.1039/C8TC05647A

Ja Lee, M., Piao, M., Jeong, M.-Y., Hae Lee, S., Min Kang, K., Jeon, S.-J., et al. (2003). Novel azo octupoles with large first hyperpolarizabilities. *J. Mat. Chem.* 13 (5), 1030–1037. Electronic supplementary information (ESI) is available: molar absorptivity spectra of 1a,d,e, P1 and P2 in THF and plots of I2ω vs. number

DATA AVAILABILITY STATEMENT

The raw data supporting the conclusion of this article will be made available by the authors, without undue reservation.

AUTHOR CONTRIBUTIONS

All authors listed have made a substantial, direct, and intellectual contribution to the work and approved it for publication.

FUNDING

ACKNOWLEDGMENTS

density for 1a,d,e and 2a,c,e in THF at 1064 nm. See http://www.rsc.org/suppdata/jm/b3/b300777d/. doi:10.1039/b300777d

Kanis, D. R., Ratner, M. A., and Marks, T. J. (1994). Design and Construction of Molecular Assemblies with Large Second-Order Optical Nonlinearities. Quantum Chemical Aspects. *Chem. Rev.* 94 (1), 195–242. doi:10.1021/cr00025a007

Karamanis, P., Otero, N., and Pouchan, C. (2014). Unleashing the Quadratic Nonlinear Optical Responses of Graphene by Confining White-Graphene (*H*-BN) Sections in its Framework. *J. Am. Chem. Soc.* 136 (20), 7464–7473. doi:10.1021/ja502631w

Koi, N., Oku, T., Narita, I., and Suganuma, K. (2005). Synthesis of Huge Boron Nitride Cages. *Diam. Relat. Mater.* 14 (3), 1190–1192. doi:10.1016/j.diamond.2004.12.018

Lee, C., Yang, W., and Parr, R. G. (1988). Development of the Colle-Salvetti Correlation-Energy Formula into a Functional of the Electron Density. *Phys. Rev. B* 37 (2), 785–789. doi:10.1103/PhysRevB.37.785

Li, J., Xia, Y., Zhao, M., Liu, X., Song, C., Li, L., et al. (2007). Theoretical Prediction for the $(AlN)_{12}$ Fullerene-like Cage-Based Nanomaterials. *J. Phys. Condens. Matter* 19 (34), 346228. doi:10.1088/0953-8984/19/34/346228

Li, Y., Li, Z.-R., Wu, D., Li, R.-Y., Hao, X.-Y., and Sun, C.-C. (2004). An Ab Initio Prediction of the Extraordinary Static First Hyperpolarizability for the Electron-Solvated Cluster $(FH)_2\{e\}(HF)$. *J. Phys. Chem. B* 108 (10), 3145–3148. doi:10.1021/jp036808y

Liu, Z.-B., Zhou, Z.-J., Li, Y., Li, Z.-R., Wang, R., Li, Q.-Z., et al. (2010). Push-pull Electron Effects of the Complexant in a Li Atom Doped Molecule with Electride Character: a New Strategy to Enhance the First Hyperpolarizability. *Phys. Chem. Chem. Phys.* 12 (35), 10562–10568. doi:10.1039/c004262e

Liu, Z., Wang, X., Liu, G., Zhou, P., Sui, J., Wang, X., et al. (2013). Low-density Nanoporous Phases of Group-III Nitrides Built from Sodalite Cage Clusters. *Phys. Chem. Chem. Phys.* 15 (21), 8186–8198. doi:10.1039/C3CP50814E

Luo, Z.-Z., Lin, C.-S., Zhang, W.-L., Zhang, H., He, Z.-Z., and Cheng, W.-D. (2014). $Ba_8Sn_4S_{15}$: A Strong Second Harmonic Generation Sulfide with Zero-Dimensional Crystal Structure. *Chem. Mat.* 26 (2), 1093–1099. doi:10.1021/cm403369m

Ma, F., Li, Z.-R., Xu, H.-L., Li, Z.-J., Li, Z.-S., Aoki, Y., et al. (2008). Lithium Salt Electride with an Excess Electron Pair-A Class of Nonlinear Optical Molecules for Extraordinary First Hyperpolarizability. *J. Phys. Chem. A* 112 (45), 11462–11467. doi:10.1021/jp8040023

Marder, S. R., Gorman, C. B., Meyers, F., Perry, J. W., Bourhill, G., Brédas, J.-L., et al. (1994). A Unified Description of Linear and Nonlinear Polarization in Organic Polymethine Dyes. *Science* 265 (5172), 632–635. doi:10.1126/science.265.5172.632

Maria, M., Iqbal, J., and Ayub, K. (2016). Theoretical Study of the Non Linear Optical Properties of Alkali Metal (Li, Na, K) Doped Aluminum Nitride Nanocages. *RSC Adv.* 6 (96), 94228–94235. doi:10.1039/C6RA21797D

Maroulis, G. (1996). Electric Properties of Carbon Tetrafluoride. *Chem. Phys. Lett.* 259 (5), 654–660. doi:10.1016/0009-2614(96)00728-2

Meyers, F., Marder, S. R., Pierce, B. M., and Bredas, J. L. (1994). Electric Field Modulated Nonlinear Optical Properties of Donor-Acceptor Polyenes: Sum-Over-States Investigation of the Relationship between Molecular Polarizabilities (.alpha., .beta., and .gamma.) and Bond Length Alternation. *J. Am. Chem. Soc.* 116 (23), 10703–10714. doi:10.1021/ja00102a040

Muhammad, S., Xu, H.-L., Zhong, R.-L., Su, Z.-M., Al-Sehemi, A. G., and Irfan, A. (2013). Quantum Chemical Design of Nonlinear Optical Materials by Sp2-Hybridized Carbon Nanomaterials: Issues and Opportunities. *J. Mat. Chem. C* 1 (35), 5439–5449. doi:10.1039/c3tc31183j

Muhammad, S., Xu, H., Liao, Y., Kan, Y., and Su, Z. (2009). Quantum Mechanical Design and Structure of the $Li@B_{10}H_{14}$ Basket with a Remarkably Enhanced Electro-Optical Response. *J. Am. Chem. Soc.* 131 (33), 11833–11840. doi:10.1021/ja9032023

Nakano, M., Fujita, H., Takahata, M., and Yamaguchi, K. (2002). Theoretical Study on Second Hyperpolarizabilities of Phenylacetylene Dendrimer: Toward an Understanding of Structure–Property Relation in NLO Responses of Fractal Antenna Dendrimers. *J. Am. Chem. Soc.* 124 (32), 9648–9655. doi:10.1021/ja0115969

Niu, M., Yu, G., Yang, G., Chen, W., Zhao, X., and Huang, X. (2014). Doping the Alkali Atom: An Effective Strategy to Improve the Electronic and Nonlinear

Optical Properties of the Inorganic $Al_{12}N_{12}$ Nanocage. *Inorg. Chem.* 53 (1), 349–358. doi:10.1021/ic4022917

Oku, T., Nishiwaki, A., and Narita, I. (2004). Formation and Atomic Structure of $B_{12}N_{12}$ Nanocage Clusters Studied by Mass Spectrometry and Cluster Calculation. *Sci. Technol. Adv. Mater.* 5 (5), 635–638. doi:10.1016/j.stam.2004.03.017

Priyadarshy, S., Therien, M. J., and Beratan, D. N. (1996). Acetylenyl-Linked, Porphyrin-Bridged, Donor–Acceptor Molecules: A Theoretical Analysis of the Molecular First Hyperpolarizability in Highly Conjugated Push–Pull Chromophore Structures. *J. Am. Chem. Soc.* 118 (6), 1504–1510. doi:10.1021/ja952690q

Saeedi, M., Anafcheh, M., Ghafouri, R., and Hadipour, N. L. (2013). A Computational Investigation of the Electronic Properties of Octahedral Al n N n and Al n P N Cages (n = 12, 16, 28, 36, and 48). *Struct. Chem.* 24 (2), 681–689. doi:10.1007/s11224-012-0119-7

Silaghi-Dumitrescu, I., Lara-Ochoa, F., and Haiduc, I. (1996). $A_{12}B_{12}$ (A = B,Al; B = N,P) Fullerene-like Cages and Their Hydrogenated Forms Stabilized by Exohedral Bonds. An AM1 Molecular Orbital Study. *J. Mol. Struct. THEOCHEM* 370 (1), 17–23. doi:10.1016/s0166-1280(96)04677-5

Srivastava, A. K., Misra, N., and Pandey, S. K. (2018). DFT Study on Planar $(CaO)_n$ Rings (N = 1-5) and Their Hydrogen Storage Behavior: Ca-O versus Mg-O Clusters. *J. Clust. Sci.* 29 (1), 57–65. doi:10.1007/s10876-017-1306-x

Stafström, S., Hultman, L., and Hellgren, N. (2001). Predicted Stability of A New aza[60]Fullerene Molecule, $C_{48}N_{12}$. *Chem. Phys. Lett.* 340 (3), 227–231. doi:10.1016/S0009-2614(01)00418-3

Strout, D. L. (2000). Structure and Stability of Boron Nitrides: Isomers of $B_{12}N_{12}$. *J. Phys. Chem. A* 104 (15), 3364–3366. doi:10.1021/jp994129a

Sun, W.-M., Li, X.-H., Wu, D., Li, Y., He, H.-M., Li, Z.-R., et al. (2016). A Theoretical Study on Superalkali-Doped Nanocages: Unique Inorganic Electrides with High Stability, Deep-Ultraviolet Transparency, and a Considerable Nonlinear Optical Response. *Dalton Trans.* 45 (17), 7500–7509. doi:10.1039/C6DT00342G

Sun, W.-M., Wu, D., Li, Y., Liu, J.-Y., He, H.-M., and Li, Z.-R. (2015). A Theoretical Study on Novel Alkaline Earth-Based Excess Electron Compounds: Unique Alkalides with Considerable Nonlinear Optical Responses. *Phys. Chem. Chem. Phys.* 17 (6), 4524–4532. doi:10.1039/C4CP04951A

Tawada, Y., Tsuneda, T., Yanagisawa, S., Yanai, T., and Hirao, K. (2004). A Long-Range-Corrected Time-dependent Density Functional Theory. *J. Chem. Phys.* 120 (18), 8425–8433. doi:10.1063/1.1688752

Ullah, F., Kosar, N., Ali, A., MariaMahmood, T., Mahmood, T., and Ayub, K. (2020). Design of Novel Inorganic Alkaline Earth Metal Doped Aluminum Nitride Complexes $(AEM@Al_{12}N_{12})$ with High Chemical Stability, Improved Electronic Properties and Large Nonlinear Optical Response. *Optik* 207, 163792. doi:10.1016/j.ijleo.2019.163792

Wang, J.-J., Zhou, Z.-J., Bai, Y., Liu, Z.-B., Li, Y., Wu, D., et al. (2012). The Interaction between Superalkalis $(M_3O, M = Na, K)$ and a $C_{20}F_{20}$ Cage Forming Superalkali Electride Salt Molecules with Excess Electrons inside the $C_{20}F_{20}$ Cage: Dramatic Superalkali Effect on the Nonlinear Optical Property. *J. Mat. Chem.* 22 (19), 9652–9657. doi:10.1039/C2JM15405F

Wang, R., Zhang, D., and Liu, C. (2005). Theoretical Prediction of a Novel Inorganic Fullerene-like Family of Silicon-Carbon Materials. *Chem. Phys. Lett.* 411 (4), 333–338. doi:10.1016/j.cplett.2005.06.055

Wang, S.-J., Wang, Y.-F., and Cai, C. (2015). Multidecker Sandwich Cluster V_nBen_{n+1}(n= 1, 2, 3, 4) as a Polarizable Bridge for Designing 1D Second-Order NLO Chromophore: Metal−π Sandwich Multilayer Structure as a Particular Charge-Transfer Axis for Constructing Multidimensional NLO Molecules. *J. Phys. Chem. C* 119 (28), 16256–16262. doi:10.1021/acs.jpcc.5b04656

Wang, X.-B., Ding, C.-F., and Wang, L.-S. (1999). High Resolution Photoelectron Spectroscopy of C_{60}^- Anions and Accurate Determination of the Electron Affinity of C_{60}. *J. Chem. Phys.* 110 (17), 8217–8220. doi:10.1063/1.478732

Wu, H.-Q., Xu, H.-L., Sun, S.-L., and Su, Z.-M. (2014). Li Doped Effect of through Novel Noncovalent Charge Transfer on Nonlinear Optical Properties. *Dyes Pigments* 106, 7–13. doi:10.1016/j.dyepig.2014.01.031

Wu, H.-S., Zhang, F.-Q., Xu, X.-H., Zhang, C.-J., and Jiao, H. (2003). Geometric and Energetic Aspects of Aluminum Nitride Cages. *J. Phys. Chem. A* 107 (1), 204–209. doi:10.1021/jp027300i

Xiao, D., Bulat, F. A., Yang, W., and Beratan, D. N. (2008). A Donor–Nanotube Paradigm for Nonlinear Optical Materials. *Nano Lett.* 8 (9), 2814–2818. doi:10.1021/nl801388z

Xu, H.-L., Li, Z.-R., Wu, D., Ma, F., Li, Z.-J., and Gu, F. L. (2009). Lithiation and Li-Doped Effects of [5]Cyclacene on the Static First Hyperpolarizability. *J. Phys. Chem. C* 113 (12), 4984–4986. doi:10.1021/jp806864w

Xu, H.-L., Li, Z.-R., Wu, D., Wang, B.-Q., Li, Y., Gu, F. L., et al. (2007). Structures and Large NLO Responses of New Electrides: Li-Doped Fluorocarbon Chain. *J. Am. Chem. Soc.* 129 (10), 2967–2970. doi:10.1021/ja068038k

Xu, X., Hu, C.-L., Kong, F., Zhang, J.-H., Mao, J.-G., and Sun, J. (2013). Cs2GeB$_4$O$_9$: a New Second-Order Nonlinear-Optical Crystal. *Inorg. Chem.* 52 (10), 5831–5837. doi:10.1021/ic302774h

Yanai, T., Tew, D. P., and Handy, N. C. (2004). A New Hybrid Exchange-Correlation Functional Using the Coulomb-Attenuating Method (CAM-B3lyp). *Chem. Phys. Lett.* 393 (1), 51–57. doi:10.1016/j.cplett.2004.06.011

Yang, Z., Shi, L., Chen, L., Gu, Y., Cai, P., Zhao, A., et al. (2005). Synthesis, Characterization and Properties of Novel BN Nanocages from a Single-Source Precursor. *Chem. Phys. Lett.* 405 (1), 229–233. doi:10.1016/j.cplett.2005.02.041

Yu, G., Zhao, X., Niu, M., Huang, X., Zhang, H., and Chen, W. (2013). Constructing a Mixed π-conjugated Bridge: a Simple and Effective Approach to Realize a Large First Hyperpolarizability in Carbon Nanotube-Based Systems. *J. Mat. Chem. C* 1 (24), 3833–3841. doi:10.1039/c3tc00022b

Zhang, D., and Zhang, R. Q. (2005). Geometrical Structures and Electronic Properties of AlN Fullerenes: A Comparative Theoretical Study of AlN Fullerenes with BN and C Fullerenes. *J. Mat. Chem.* 15 (29), 3034–3038. doi:10.1039/B503724G

Zhang, Q., Chung, I., Jang, J. I., Ketterson, J. B., and Kanatzidis, M. G. (2009). Chalcogenide Chemistry in Ionic Liquids: Nonlinear Optical Wave-Mixing Properties of the Double-Cubane Compound [Sb7S8Br$_2$](AlCl$_4$)$_3$. *J. Am. Chem. Soc.* 131 (29), 9896–9897. doi:10.1021/ja903881m

Zhang, T.-G., Zhao, Y., Asselberghs, I., Persoons, A., Clays, K., and Therien, M. J. (2005). Design, Synthesis, Linear, and Nonlinear Optical Properties of Conjugated (Porphinato)Zinc(II)-Based Donor–Acceptor Chromophores Featuring Nitrothiophenyl and Nitrooligothiophenyl Electron-Accepting Moieties. *J. Am. Chem. Soc.* 127 (27), 9710–9720. doi:10.1021/ja0402553

Zhong, R.-L., Xu, H.-L., Li, Z.-R., and Su, Z.-M. (2015). Role of Excess Electrons in Nonlinear Optical Response. *J. Phys. Chem. Lett.* 6 (4), 612–619. doi:10.1021/jz502588x

Zhong, R.-L., Xu, H.-L., Muhammad, S., Zhang, J., and Su, Z.-M. (2012a). The Stability and Nonlinear Optical Properties: Encapsulation of an Excess Electron Compound LiCN···Li within Boron Nitride Nanotubes. *J. Mat. Chem.* 22 (5), 2196–2202. doi:10.1039/C1JM14358A

Zhong, R.-L., Xu, H.-L., Sun, S.-L., Qiu, Y.-Q., and Su, Z.-M. (2012b). The Excess Electron in a Boron Nitride Nanotube: Pyramidal NBO Charge Distribution and Remarkable First Hyperpolarizability. *Chem. Eur. J.* 18 (36), 11350–11355. doi:10.1002/chem.201201570

Zhou, Z.-J., Yu, G.-T., Ma, F., Huang, X.-R., Wu, Z.-J., and Li, Z.-R. (2014). Theoretical Investigation on Nonlinear Optical Properties of Carbon Nanotubes with Stone-Wales Defect Rings. *J. Mat. Chem. C* 2 (2), 306–311. doi:10.1039/c3tc31904k

Zope, R. R., and Dunlap, B. I. (2005). Electronic Structure of Fullerenelike Cages and Finite Nanotubes of Aluminum Nitride. *Phys. Rev. B* 72 (4), 045439. doi:10.1103/PhysRevB.72.045439

Conflict of Interest: The authors declare that the research was conducted in the absence of any commercial or financial relationships that could be construed as a potential conflict of interest.

Publisher's Note: All claims expressed in this article are solely those of the authors and do not necessarily represent those of their affiliated organizations, or those of the publisher, the editors, and the reviewers. Any product that may be evaluated in this article, or claim that may be made by its manufacturer, is not guaranteed or endorsed by the publisher.